Available online at www.sciencedirect.com
ScienceDirect
Cement and Concrete Research 37 (2007) 978–987
Cement and Concrete Research

Phase distribution and microstructural changes of self-compacting cement paste at elevated temperature

G. Ye [a,d,*], X. Liu [b], G. De Schutter [a], L. Taerwe [a], P. Vandevelde [c]

[a] Magnel Laboratory for Concrete Research, Department of Structural Engineering, Ghent University, Belgium
[b] School of Civil Engineering, Tongji University, Shanghai, China
[c] Laboratory for Fire Research, Department of Structural Engineering, Ghent University, Belgium
[d] Microlab, Faculty of Civil Engineering and Geosciences, Delft University of Technology, Delft, The Netherlands

Received 14 February 2005; accepted 7 February 2007

Abstract

Self-compacting concrete, as a new smart building material with various advanced properties, has been used for a wide range of structures and infrastructures. However little investigation have been reported on the properties of Self-compacting when it is exposed to elevated temperatures. Previous experiments on fire test have shown the differences between high performance concrete and traditional concrete at elevated temperature. This difference is largely depending on the microstructural properties of concrete matrix, i.e. the cement paste, especially on the porosity, pore size distribution and the connectivity of pores in cement pastes.

In this contribution, the investigations are focused on the cement paste. The phase distribution and microstructural changes of self-compacting cement paste at elevated temperatures are examined by mercury intrusion porosimetry and scanning electron microscopy. The chemical decomposition of self-compacting cement paste at different temperatures is determined by thermogravimetric analysis. The experimental results of self-compacting cement paste are compared with those of high performance cement paste and traditional cement paste. It was found that self-compacting cement paste shows a higher change of the total porosity in comparison with high performance cement paste. When the temperature is higher than 700 °C, a dramatic loss of mass was observed in the self-compacting cement paste samples with addition of limestone filler. This implies that the SCC made by this type of self-compacting cement paste will probably show larger damage once exposed to fire. Investigation has shown that 0.5 kg/m^3 of Polypropylene fibers in the self-compacting cement paste can avoid the damage efficiently.

Keywords: Phase distribution; Self-compacting cement paste; Microstructure; Porosity; Temperature

1. Introduction

Self-compacting concrete (SCC), as a building material with high flowability, good mechanical properties and easy casting without vibration, has been used for a wide range of structures and infrastructures [1–3]. SCC often incorporates limestone filler or fly ash to ensure high fluidity and to reduce the water/cement ratio (w/c).

A compilation of fire test data has shown distinct behavioural differences between high performance concrete (HPC) and traditional concrete (TC) at elevated temperature [4,5]. The concrete mixture of HPC is made with lower water cement ratio and superplasticizer is normally added in order to improve the workability. The differences of HPC and TC in fire behaviour depend largely on the microstructure properties [6,7]. However, most of the fire research focuses on large scale specimens and only a few researchers [5] paid attention to the phenomenon of microstructural change, for example, the changes of porosity, pore size distribution and connectivity of pores. As pointed out in [5], due to the lower porosity and lower connectivity of pores in high performance cement paste, the accumulating moisture and water vapour can hardly escape from the structure. This leads to more serious problems in a

* Corresponding author. Microlab, Faculty of Civil Engineering and Geosciences, Delft University of Technology, Delft, The Netherlands. Tel.: +31 15 2784001; fax: +31 15 2786383.
E-mail address: ye.guang@citg.tudelft.nl (G. Ye).

0008-8846/$ - see front matter © 2007 Elsevier Ltd. All rights reserved.
doi:10.1016/j.cemconres.2007.02.011

Table 1
The chemical and physical properties of cement and limestone powder [8]

	CEM I 52.5 (%)	Limestone filler (%)
CaO	63.95	–
SiO_2	20.29	0.80
Al_2O_3	4.52	0.17
Fe_2O_3	2.35	0.10
MgO	2.22	0.50
K_2O	0.94	–
Na_2O	0.20	–
SO_3	3.35	–
Cl^-	0.015	0.002
$CaCO_3$	–	98.00
C_3S	59.0	–
C_2S	12.60	–
C_3A	8.01	–
C_4AF	9.40	–

high performance concrete structures under fire conditions than in traditional concrete.

It is clear that the properties of concrete are different compared to cement paste due to the influence of the interface zone. However, when concrete is exposed to fire, the microstructure change and the decomposition of cement matrix are the main reasons for causing fire spalling [5–7]. Investigation on the paste level can also avoid difficulties due to presence of aggregate in the experimental program in observing the microstructural change. In this research, without specification, the specimens of self-compacting cement paste (SCCP), high performance cement paste (HPCP) and traditional cement paste (TCP) were having the same mix proportions as SCC, HPC and TC, however without any aggregate. Recent research [10,11] has shown that at the same water/powder ratio, the porosity and pore size distribution of self-compacting cement paste are very similar to that of high performance cement paste. This suggests that when self-compacting concrete is exposed to elevated temperatures, it might have the same risk (i.e. explosive spalling) as high performance concrete. However, the phase composition of SCCP and HPCP is different as observed by scanning electron microscopy and DTA/TGA measurements [10]. In the case of limestone as filler in SCCP, the limestone particles only decompose at a temperature of 700 °C and the weight loss of SCCP is much smaller than that of HPCP below this temperature.

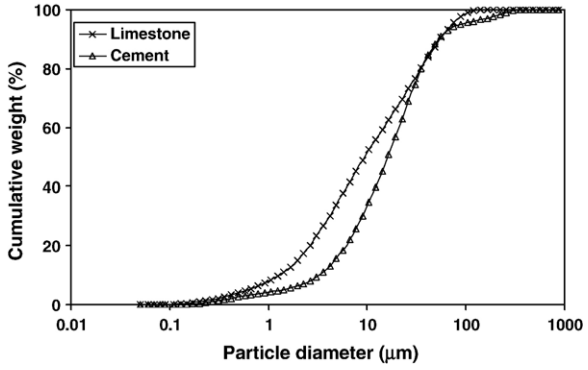

Fig. 1. Particle size distribution of cement and limestone [8].

Polypropylene fibers (PPF) have been shown to reduce the damage to high performance concrete structures at elevated temperatures [5–9] and widely been used in construction industry. However, the mechanism and the microstructural changes influenced by PPF are still unclear.

The purpose of this research was the identification of the microstructural changes of SCCP at elevated temperatures, with and without PPF. The microstructural properties, i.e., porosity, pore size distribution and phase distribution were measured. To this end, mercury intrusion porosimetry has been performed on self-compacting cement paste, high performance cement paste and traditional cement paste at different curing ages. Meanwhile, scanning electron microscopy was employed to examine the phase distribution (pore, CSH, $Ca(OH)_2$ and unhydrated cement core) at the same curing age. The chemical decomposition of self-compacting cement paste at different temperatures is determined by thermogravimetric analysis. The influence of amount of PPF on the microstructural change was considered. The experimental results of SCCP are compared with HPCP and TCP. Based on the investigation of microstructural change at elevated temperature on paste level, a fundamental understanding of fire behaviour of concrete is expected.

2. Materials and methods

2.1. Materials

The SCCP mixtures used in this study were prepared with Portland cement I 52.5, with limestone powder added as filler. The limestone powder was produced from carboniferous limestone of a very high purity (98% of $CaCO_3$ content). The chemical and physical properties of cement and limestone powder are presented in Table 1.

The particle size distribution of Portland cement and limestone are shown in Fig. 1. The Blaine value of limestone and CEM I 52.5 are 526 m^2/kg and 420 m^2/kg respectively. The average particle size of limestone filler is slightly smaller than that of Portland cement CEM I 52.5.

2.2. Mixture design and specimens casting

2.2.1. Mixture design

The mix proportions of SCCP, HPCP and TCP without PPF are listed in Table 2. Two kinds of SCCP with varied amount of

Table 2
Mix proportions of four cement pastes (kg/m^3)

	TCP	SCCP		HPCP
	Mix01	Mix02	Mix03	Mix04
Portland cement I 52.5	350	400	400	400
Water	165	165	132	132
Limestone powder	–	200	300	–
Glenium 51 (liter)	–	3.2	2.7	–
Rheobuild	–	–	–	8.45
Total powder content		600	700	400
Water/cement ratio	0.48	0.41	0.48	0.33
Water/powder ratio	0.48	0.28	0.27	0.33

Table 3
Mix proportions of SCCP, and HPCP with PPF (kg/m^3)

	SCCP				HPCP	
	MIX02PPF05	MIX02PPF1	MIX03PPF05	MIX03PPF1	MIX04PPF05	MIX04PPF1
Portland cement I 52.5	400	400	400	400	400	400
Water	165	165	192	192	132	132
Limestone powder	200	200	300	300	–	–
Glenium 51 (liter)	*4.42*	*5.55*	*3.25*	*3.5*	–	–
Superplasticizer	–	–	–	–	*7.0*	*8.45*
PP fibers	0.5	1	0.5	1	0.5	1
Total powder content	600	600	700	700	400	400
Water/cement ratio	0.41	0.41	0.48	0.48	0.33	0.33
Water/powder ratio	0.28	0.28	0.27	0.27	0.33	0.33

limestone powder were considered in this study. In order to compare with TCP, SCCP Mix03 had same w/c ratio (0.48) as TCP. Different PPF dosages were used in the SCCP and HPCP mixtures. Table 3 lists the mix proportions of samples made with PPF at the dosage of 0.5 and 1 kg/m^3. The PPF have a length of 12 mm and a diameter of 18 μm. Due to the PPF added in the SCCP and HPCP mixtures, the total amount of superplasticizer had to be increased in order to obtain the same workability as the SCCP or HPCP mixtures made without PPF. Two different superplastisizers were used, in agreement with common practise in industry. A polycarbonalate was used for SCCP, while a non-traditional naphtalene sulphonate was used for HPCP.

2.2.2. Specimens casting and curing

First, cement was mixed with water for 2 min at lower speed in a horizontal pan mixer with a normal capacity of 5 l. Afterwards, the superplasticizer was added and the paste was mixed for another 3 min at high speed. After mixing, the cement pastes were immediately cast into 1000 ml plastic bottles. The plastic bottles were rotated at a speed of 5 rpm in a room with temperature of 20 °C. After 24 h of rotation, the samples were still kept in the plastic bottle and stored in the curing room with temperature of 20 °C until the age of testing. The rotational procedure avoids the influence of bleeding on the pore structure in cement paste [12]. At different age, the sample was removed from the plastic bottle and dried in an oven at 105 °C till constant weight. The weight loss of the samples was recorded.

The specimens for the fire test were cast in a wooden mould with a size of 175 × 90 × 100 mm. Four hours after casting, the samples were sealed with aluminium paper to prevent moisture loss and cured in container at a temperature of 20 °C.

2.3. Techniques and procedures

All samples were exposed to elevated temperatures in an electrical resistance furnace at a heating rate of 10 °C/min. The maximum temperature reached in the furnace was 950 °C. The temperature histories were monitored by a K type thermo-couple at the surface of the specimens and in the specimens at a distance of 10, 20 and 30 mm from the exposed surface. After the furnace reached the maximum temperature, it was switched off and the samples were left in the furnace until they cooled to ambient temperature. The degree of damage on the surface of the samples was observed and photographed. The specimens were split and samples were taken from places at 10, 20 and 30 mm from the exposed surface and were stored in a dessicator.

An example of temperature history of SCCP MIX02 tested at 28 days is shown in Fig. 2.

After one and a half hours, the surface temperature reached 950 °C. At 10 mm from the exposed surface, the maximum temperature is reduced to about 470 °C. At a depth of 20 and 30 mm, maximum temperatures of 350 and 300 °C respectively, can be observed. The maximum values depend on the type of specimen and the curing age. The maximum temperatures for the specimens without PPF at 28 days are listed in Table 4.

Mercury porosimeter testing was performed for all samples. The maximum pressure of the PMI automated porosimeter is 420 MPa. In order to avoid the influence of higher pressures damaging the CSH gel structure, the highest pressure used in the experiments was 212 MPa. The surface tension of mercury is 480×10^{-3} N/m and the contact angle was 140°. According to Washburn equation, a minimum pore diameter of 0.0069 μm can be accessed. The technical parameters deduced from mercury porosimeter testing include total porosity, pore size distribution, median pore diameter and threshold pore diameter [12]. The threshold pore diameter is defined as the peak corresponding to the higher rate of mercury intrusion per change in pressure [13].

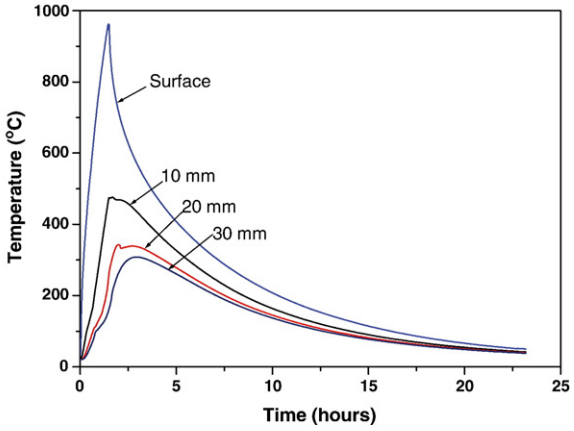

Fig. 2. Temperature history of SCCP MIX02 at 28 days.

Table 4
The maximum temperatures for the different specimens at 28 days

	Mix02				Mix03				Mix04			
Distance from surface (mm)	0	10	20	30	0	10	20	30	0	10	20	30
Maximum temperature (°C)	956	470	350	300	960	496	436	285	952	446	376	285

In this study, thermal analysis by the TGA and DTA was performed for the samples before and after exposure to elevated temperature at an age of 28 days (TA Instruments 2960 SDT V3.0F, 10 °C/min, up to 1200 °C, at atmospheric pressure, in nitrogen). Backscattered electron microscopy was employed to identify the phase distribution. In order to obtain high quality image using a backscattered electron detector, the samples have to be prepared carefully, including epoxy impregnation, cutting, grinding and polishing. The procedure was extensively described in [12]. In order to make a quantitative comparison between different samples, a "pore size" and pore size distribution technique for 2D backscatter image analysis was used [12]. The area of the feature on the polished surface of image was assessed by multiplying the number of pixels contained in the feature by the area per pixel. The equivalent diameter of a circle of area equal in area to that of the feature was calculated, the cumulative pore area fraction against equivalent pore diameter was obtained.

3. Results and discussion

3.1. Outlook of the surface of the samples after exposure to elevated temperature

Following exposure to high temperature, none of the specimens showed signs of explosive spalling. Inspection of the exposed surface following the test showed map-cracking on the surface of all the specimens. This is due to the small size of the samples and low heating rate. The surfaces of four samples are illustrated in Fig. 3. It is observed that SCCP samples show a somewhat different crack pattern compared with TCP and HPCP. The crack in SCCP samples are distributed uniformly, while several wider cracks can be found in samples of TCP and HPCP.

3.2. Mercury intrusion porosimetry (MIP) measurements

3.2.1. Microstructure of the samples without PPF after heating

The mercury intrusion porosimetry results of four mixtures without PPF at depths of 10, 20 and 30 mm, after heating, are shown in Fig. 4. In Fig. 4, the reference is the MIP result of the unexposed reference samples.

The change of total porosity is used as a parameter to compare the change of the microstructure during heating. It is defined as the total porosity increase after heat exposure divided by the total porosity of the reference samples (not heated). The results of four mixtures are shown in the left part of Fig. 5a. From Figs. 4 and 5a, it is obvious that the closer to the heated face, the greater the change of the total porosity. The threshold pore diameter also increases closer to the heated face. A 180% of total porosity change can be found in MIX02 at 10 mm of the heated face. The critical pore diameter of sample MIX02 changes from 0.1 μm to 1 μm. As shown in Fig. 4b, the temperature reached at this position (10 mm) was around 450 °C. At this temperature the

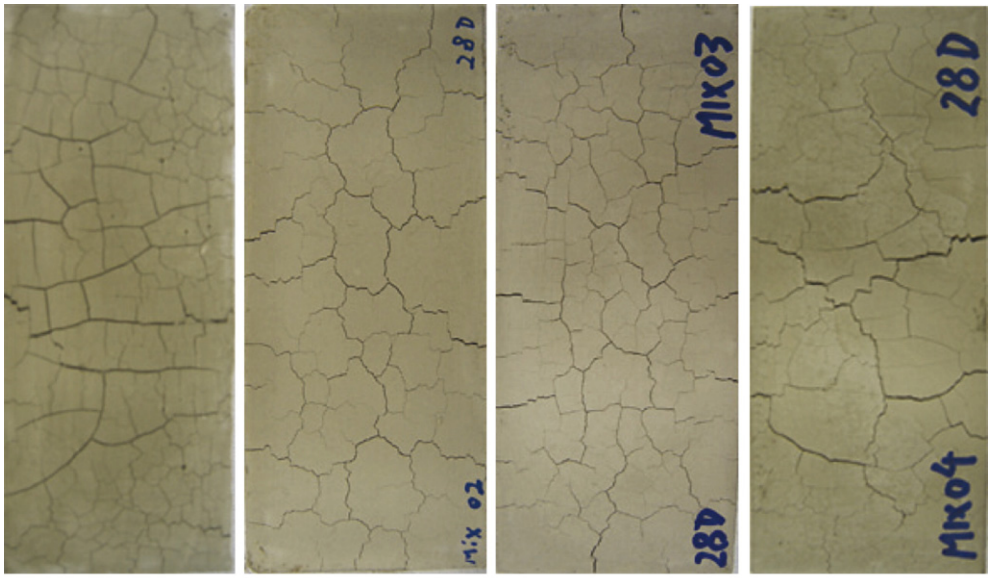

(a) MIX01 (TCP) **(b)** MIX02 (SCCP) **(c)** MIX03(SCCP) **(d)** MIX04 (HPCP)

Fig. 3. Photography of four mixtures after heating to 950 °C at curing age of 28 days.

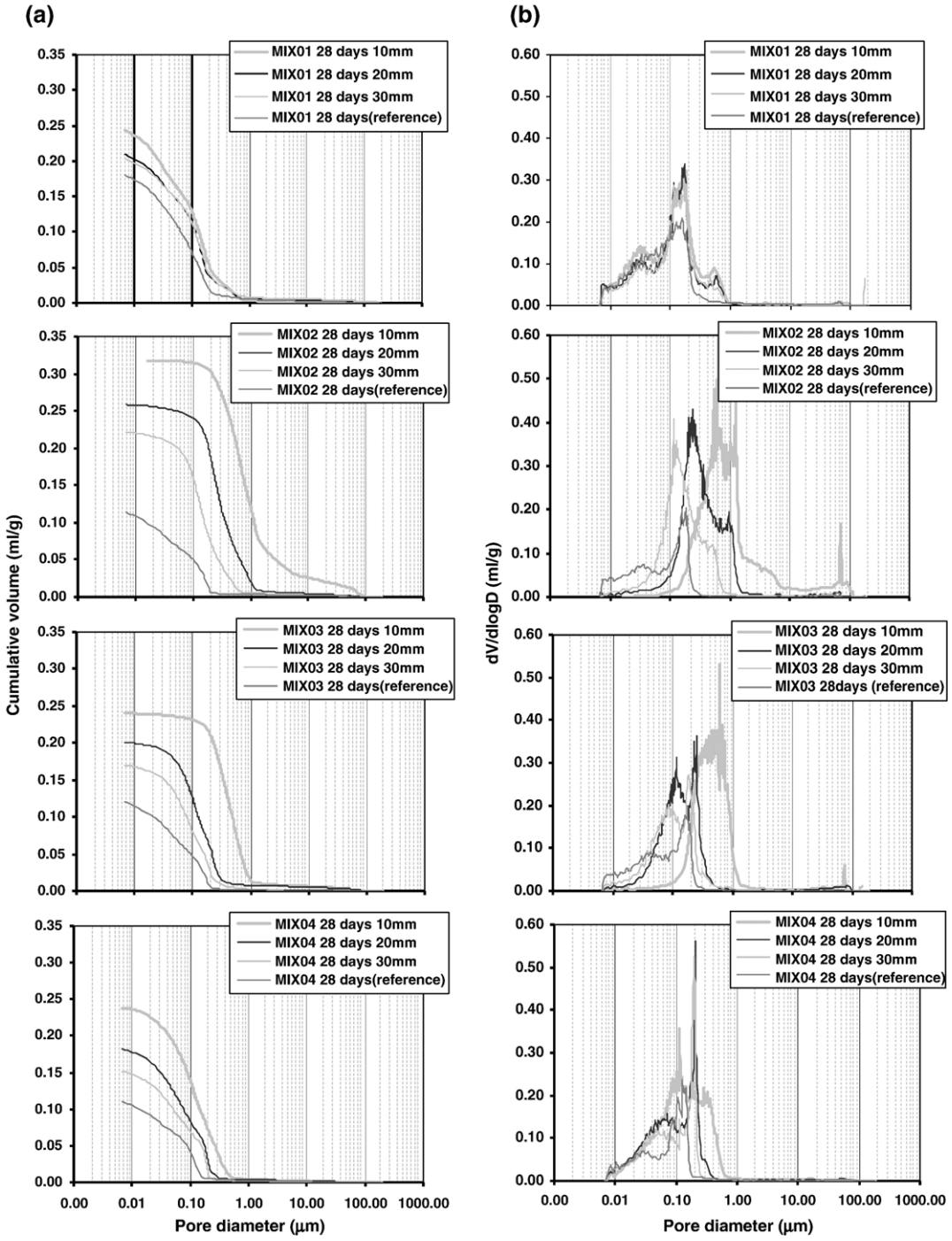

Fig. 4. MIP results of four mixtures at different layers after exposure to heating and reference specimens.

main hydration products, C–S–H and CH have been decomposed [6]. This results in an additional void space.

From Fig. 5a, it can be observed that the change of the total porosity at the same depth is different for the different mixtures. The sample made with TCP shows a lower porosity change than SCCP and HPCP.

3.2.2. Microstructure of the samples with PPF after heating

The influence of PPF on the change of microstructure at different depth for SCCP samples (MIX02) determined by MIP is shown in detail in Fig. 6 and summarized in Fig. 5b. The median pore diameter of the samples after heating is given in Table 5.

It appears that the microstructure of SCCP after heating is much influenced by the presence of PPF in the mixtures. This can be seen from both Figs. 5b and 6, where the change of total porosity decreases with increasing PPF content. The same tendency can be found in all samples at the three different depths. It cal also be seen that the increase in median pore diameter (Table 5) is smaller with increasing PPF content. The median pore

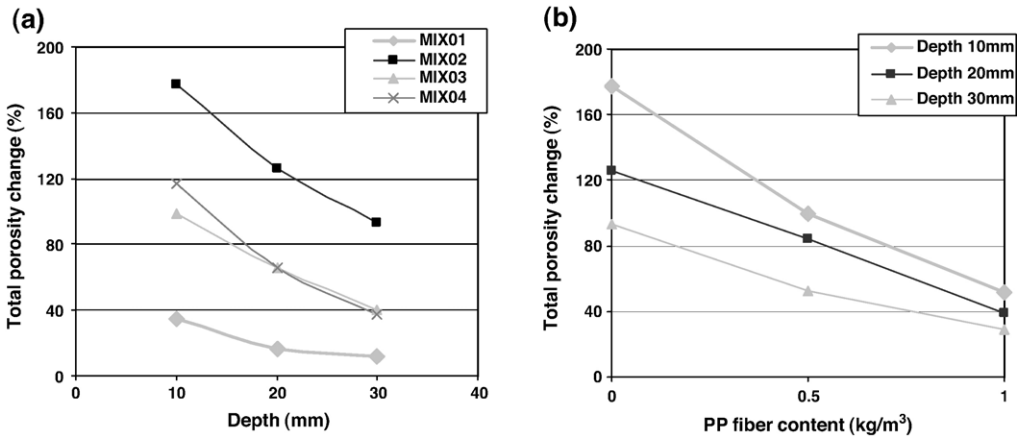

Fig. 5. Change of the total porosity after heating of four mixtures without PPF at 28 days (a), SCCP MIX02 with PPF at 28 days at different depths after heating (b).

diameter of the sample with 1 kg/m^3 PPF at 20 mm is 0.0952 μm, which is a very small change compared to the reference sample (not heated), where the median pore diameter is 0.0814 μm.

1 kg/m^3 of PPF in the SCCP reduces the change of total porosity by a factor of 3 at all depths. This is in agreement with previous fire tests by Persson [7] where 0.7 kg/m^3 18 μm PPF

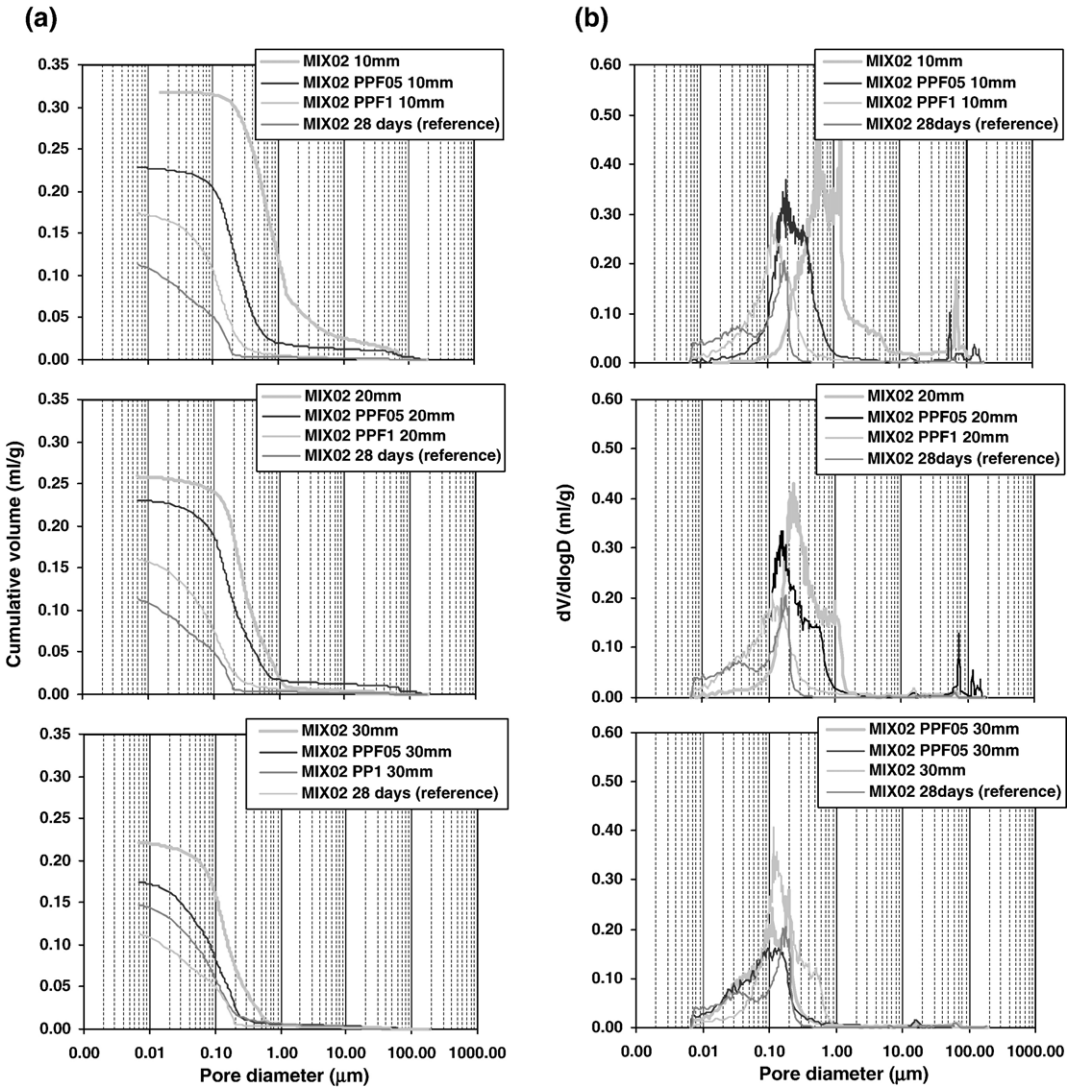

Fig. 6. Influence of PPF on the MIP results of SCCP at different depths after exposure to heating and comparison with the reference samples.

Table 5
Median pore diameter (μm) of MIX02 containing different amounts of PPF after heating

	MIX02PPF0	MIX02PPF05	MIX02PPF1	Reference
10 mm from exposed face	0.7586	0.2350	0.1199	0.0814
20 mm from exposed face	0.2915	0.1898	0.0952	0.0814
30 mm from exposed face	0.1465	0.0986	0.0816	0.0814

can effectively prevent fire spalling of SCCP, even after rapid heating.

The reason why PPF can reduce the damage of the microstructure when cement paste is exposed to fire can be explained from BSE image analysis. Fig. 7a shows an example of a BSE image of the sample MIX02 with 1 kg/m^3 PPF content at 30 mm from the heated surface and gives a comparison with the sample made without PPF (Fig. 7b). Obviously, a long pore with diameter around 20 μm can be found in Fig. 7b. Besides, there are quite a number of small pores distributed almost uniformly in the same sample with PPF after fire. These pores are the remaining PPF which melt at 171 °C. The pores resulting from melting of the PPF can be considered as a connected pore system in which the heat and water vapour can escape from the

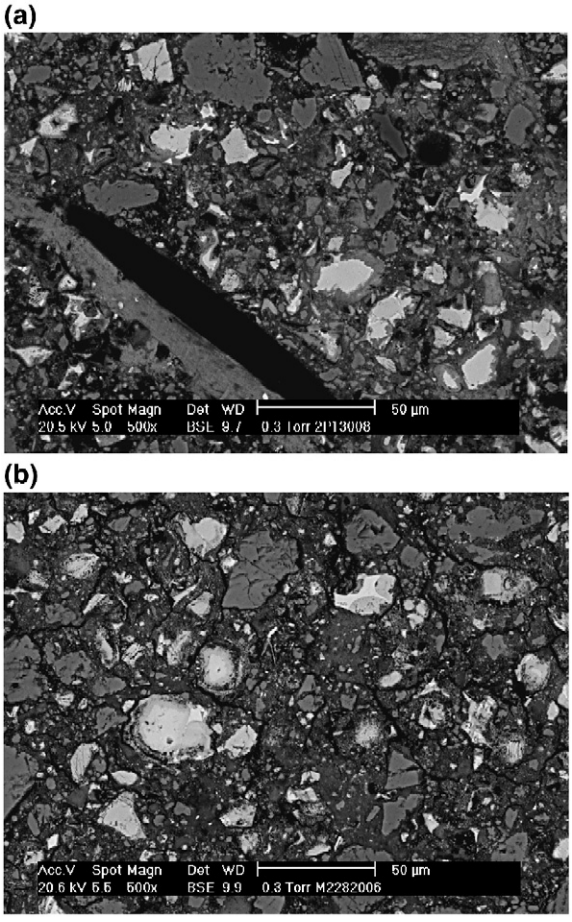

Fig. 7. BSE images of the samples with (a) and without (b) PPF after fire.

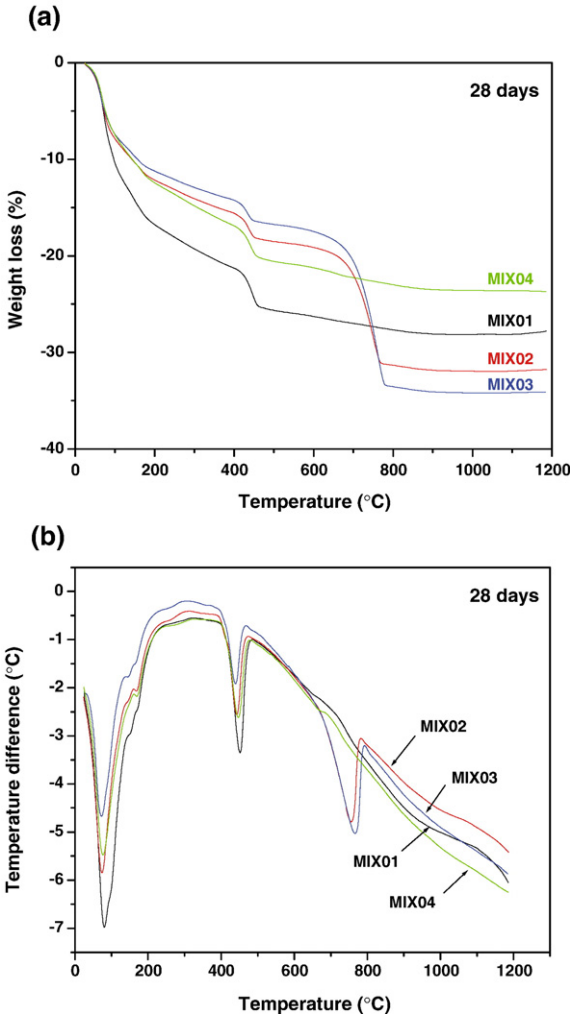

Fig. 8. (a) The thermal decomposition of the cement paste by the thermogravimetric analysis (TGA) and (b) the derivative thermogravimetric analysis (DTG) of four samples.

inside of the cement paste. This avoids further damage of the microstructure due to release of the internal pressure [5,7]. On the contrary, a lot of cracks can be observed from the sample without PPF as shown in Fig. 7b.

3.3. Thermal analysis

Thermo-analytic techniques, including thermogravimetric analysis (TGA) and differential thermogravimetry (DTA), have been used successfully to determine the temperature history of cement paste after fire exposure. Different authors [14–16] have described the reactions that occur with an increase of temperature in cement paste. Along the temperature history, the release of adsorbed water, gel water release and the decomposition of portlandite will take place.

In this study, thermal analysis by the TGA and DTA were performed for the samples with and without PPF at an age of 28 days. The samples include unheated sections as reference and the heated ones. Results for 4 cement pastes without PPF are shown in Fig. 8 and with 1 kg/m^3 PPF are shown in Fig. 9.

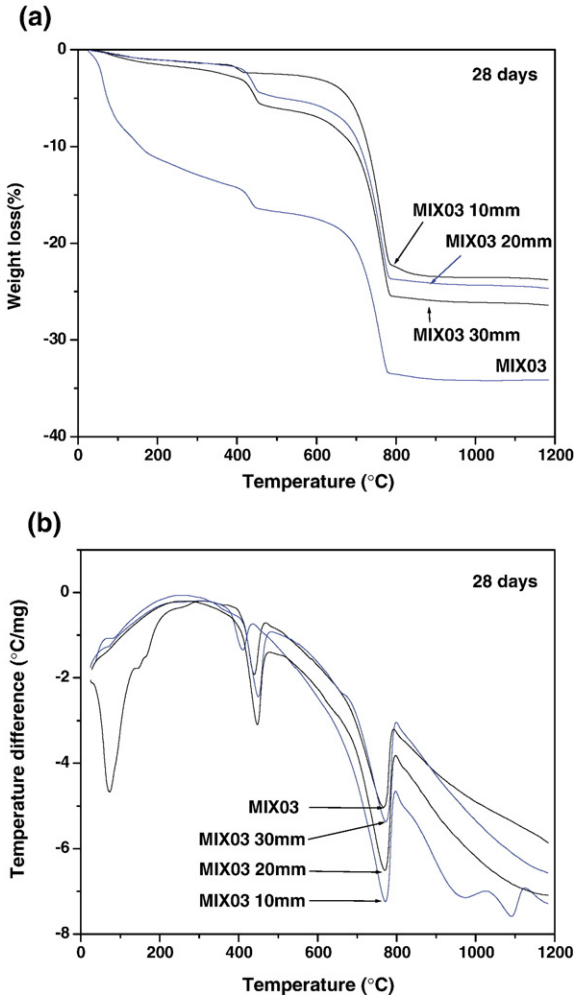

Fig. 9. TGA (a) and DTG (b) curve for the sample MIX03 after heating.

Between 30 and 150 °C, a quick weight loss was found in the TGA for all samples, especially the sample made with TCP. This corresponds to the loss of the evaporable water and part of the physically bound water [6] as can be seen from the water content shown in Table 6, where the sample made with TCP has a higher water content (21%) than the others. This is in good agreement with the observation by Bazant and Kaplan [6].

From 110 to 700 °C, the weight loss indicated from TGA includes the loss of chemically bound water from the decomposition of the CSH, the carboaluminate hydrates and the dehydroxylation of CH [6]. It can be observed that the samples made with SCCP show much less weight loss than the sample made with TCP and even less than the sample made with HPCP. This is due to the fact that the SCCP had much less hydration products as can been seen from the investigation by

Table 6
Water content of 4 mixtures at 28 days (mass percentage)

Samples	MIX01	MIX02	MIX03	MIX04
28 days	20.95	14.03	13.05	13.43

Table 7
Phase distribution (in volume percentage) of 4 mixtures at 28 days

	Porosity	C–S–H	CH	$CaCO_3$	Unhydrated cement	(C–S–H+CH)/cement content
MIX01 28 days	14.26	48.40	27.32	–	10.02	0.192
MIX02 28 days	9.32	46.07	21.20	16.94	6.47	0.168
MIX03 28 days	11.96	42.13	22.36	17.37	6.18	0.111
MIX04 28 days	8.53	56.32	25.70	–	9.45	0.205

BSE image analysis (see Table 7). This is confirmed from total hydration products (C–S–H+CH) normalize to the cement content as shown in Table 7, where ratios of hydration products to the total cement content for Mix02 and Mix03 are 0.168 and 0.111 and for TCP and HPCP are 0.192 and 0.205 respectively.

The weight loss of the samples made with SCCP is lower than the others for temperatures up to 700 °C. However, when the temperature is higher than 700 °C, a dramatic loss of weight was observed from TGA in both SCCP samples. This is due to

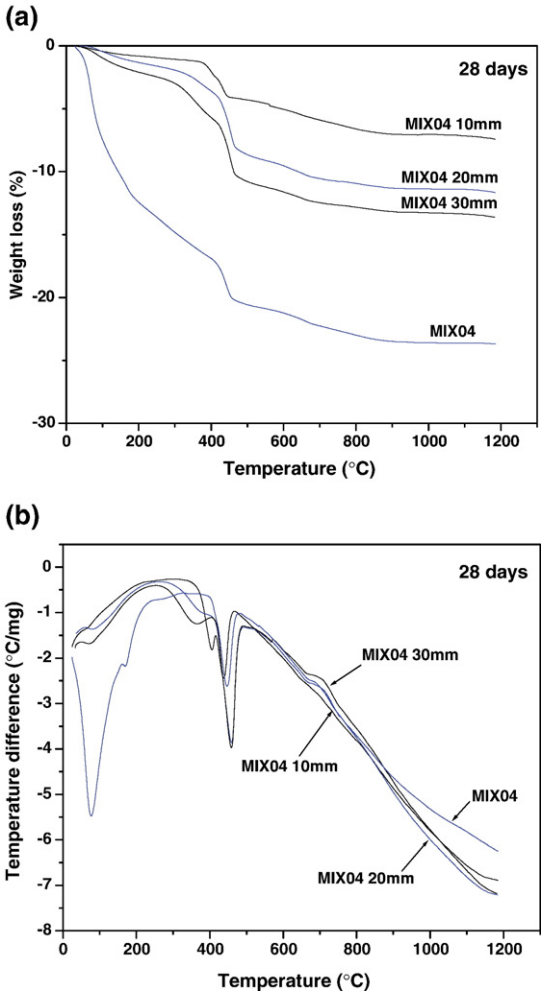

Fig. 10. TGA (a) and DTG (b) curve for the sample MIX04 after heating.

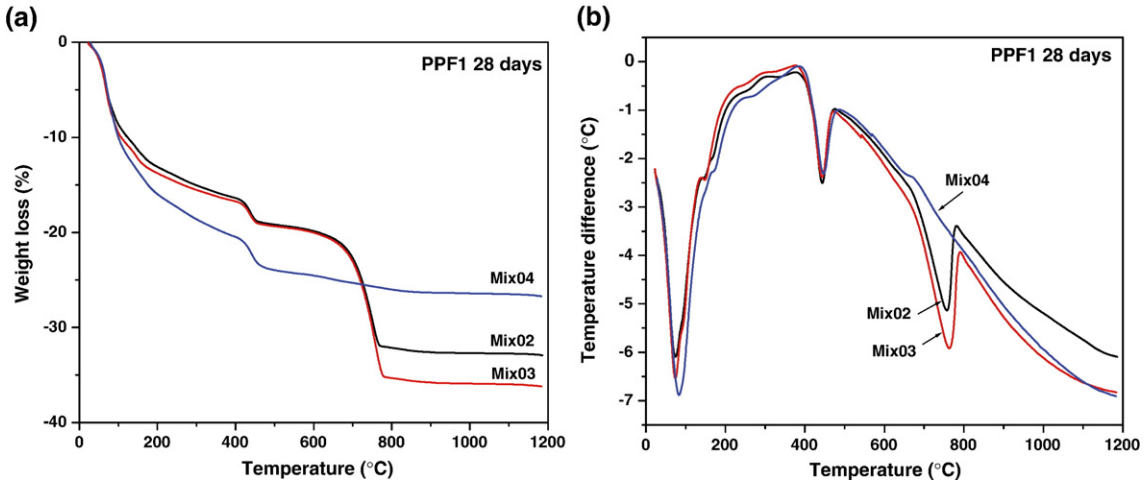

Fig. 11. (a) The thermal decomposition of the cement paste by TGA and (b) DTG of three samples with PPF.

the decomposition of carboniferous limestone filler, i.e. $CaCO_3 \rightarrow CaO + CO_2$ [6].

The thermal decomposition of the samples after heating from MIX03 and MIX04 after heating, at 10, 20 and 30 mm from the heated surface, is shown in Figs. 9 and 10 respectively. For both MIX03 and MIX04, the first peak at 100 °C has disappeared in the DTG curves. The free water has already evaporated during heating.

Significant differences can be found in the step around 400 and 750 °C. Most portlandite has been decomposed at 10 mm from the heated surface, especially for SCCP samples. Changes in temperature of decomposition show that at all depths from the heating surface, the carboniferous did not decompose even at 10 mm from the heating surface.

4. Conclusions

The microstructure of various constituents after exposure to heat was investigated by MIP, TGA/DTA and BSE imaging technique. The major results obtained in this study are as follows:

1) The total porosity and the threshold pore diameter increase in the direction of the heating face. The total porosity increases by a factor of 2 and the critical pore diameter increases by a factor of 10 at 10 mm depth for SCCP mixtures.
2) According to different water/powder ratio, self-compacting cement paste shows a higher change or at least the same change of the total porosity in comparison with HPCP. Once SCC and HPC made with SCCP and HPCP, the SCC could show to some extent similar damage as HPC under fire exposure.
3) From a detailed investigation on the samples at different depth from heating surface, it was found that the total porosity decreases with increasing PPF content (see Fig. 11). Presence of PPF can reduce the damage of microstructure as the melted PPF form a connected pore system in which the heat and water vapour can escape from inside of the specimens. Investigation has shown that 0.5 and 1 kg/m^3 of PPF in the SCCP can already avoid the damage efficiently.
4) TGA/DTA experiments indicate that the SCCP samples show a better stability below 700 °C due to low cement content in the mixtures. However, when the temperature is higher than 700 °C, a dramatic loss of mass was observed in the SCCP samples with addition of limestone filler. This also implies that this type of SCC made with SCCP will probably show larger damage once exposed to fire.

Acknowledgements

The research was financially supported by the Fund for Scientific Research — Flanders (Belgium) (FWO), which is gratefully acknowledged. The technical support during MIP measurements from the company PMI (Porous Materials, Inc.) is also appreciated.

References

[1] Y. Akkaya, A. Ilki, M.A. Tasdemir, N. Kumbasar, Self-compacting cement paste for light-weight slabs, First North American Conference on the Design and Use of Self-Consolidating Concrete, Nov. 12–13, 2002, ACBM Publication, 2002, pp. 457–468.
[2] J. Bickley, K.H Khayat, M. Lessard, Performance of self-consolidating Concrete for casting basement and foundation walls, ACI Mater. J. 97 (3) (2000) 374–380.
[3] P. Billberg, O. Petersson, T. Osterberg, Casting of three bridges with self-compacting Concrete, Nord. Concr. Res. (1999) 91–93.
[4] B. Persson, Fire resistance of self-compacting Concrete, SCC, Mat. Struct. 37 (273) (2004) 575–584.
[5] P. Kalifa, F.D. Menneteau, D. Quenard, Spalling and pore pressure in HPC at high temperatures, Cem. Concr. Res. 30 (12) (2000) 1915–1927.
[6] Z.P. Bazant, M.F. Kaplan, Concrete at High Temperatures, Longman — Addison-Wesley, London, 1996.
[7] P. Kalifa, G. Chéné, Ch. Gallé, High-temperature behaviour of HPC with polypropylene fibres: from spalling to microstructure, Cem. Concr. Res. 31 (10) (2000) 1487–1499.
[8] L.T. Phan, J.R. Lawson, F.L. Davis, Effects of elevated temperature exposure on heating characteristics, spalling, and residual properties of high performance concrete, Mater. Struct. 34 (2001) 83–91.
[9] B. Persson, Mitigation of the fire spalling of concrete with fibres, Presentation in RILEM technical committee "Durability of Self-compacting Concrete", Gent (Belgium), April 2005.

[10] G. Ye, X. Liu, G. de Schutter, A.M. Poppe, L. Taerwea, Influence of limestone powder used as filler in SCC on hydration and microstructure of cement pastes, on Cem. Concr. Res. 29 (2) (2007) 94–102.
[11] A. M. Poppe, Influence of filler on hydration and properties of self-compacting Concrete. (In Dutch), PhD thesis, University of Ghent, Gent, 2004.
[12] G. Ye, Experimental study and numerical simulation of the development of the microstructure and permeability of cementitious materials, PhD thesis, Delft University of Technology, Delft, 2003.
[13] L. Cui, J.H. Cahyadi, Permeability and pore structure of OPC paste, Cem. Concr. Res. 31 (2) (2001) 277–282.
[14] S. Kakali, Tsivilis, A. Tsialtas, Hydration of Ordinary Portland cements made from raw mix containing transition element oxides, Cem. Concr. Res. 28 (3) (1998) 335–340.
[15] E.T. Stepkowska, J.M. Blanes, F. Franco, C. Real, J.L. Pérez-Rodríguez, Phase transformation on heating of an aged cement paste, Thermochim. Acta 420 (1–2) (2004) 79–87.
[16] P.M. Buchler, A.C. Viera-coelho, F.K. Cartledge, J. Dweck, Hydration of a portland cement blended with calcium carbonate, Thermochimica Acta, vol. 346, Belfast, Irlanda, 2000, pp. 105–113.